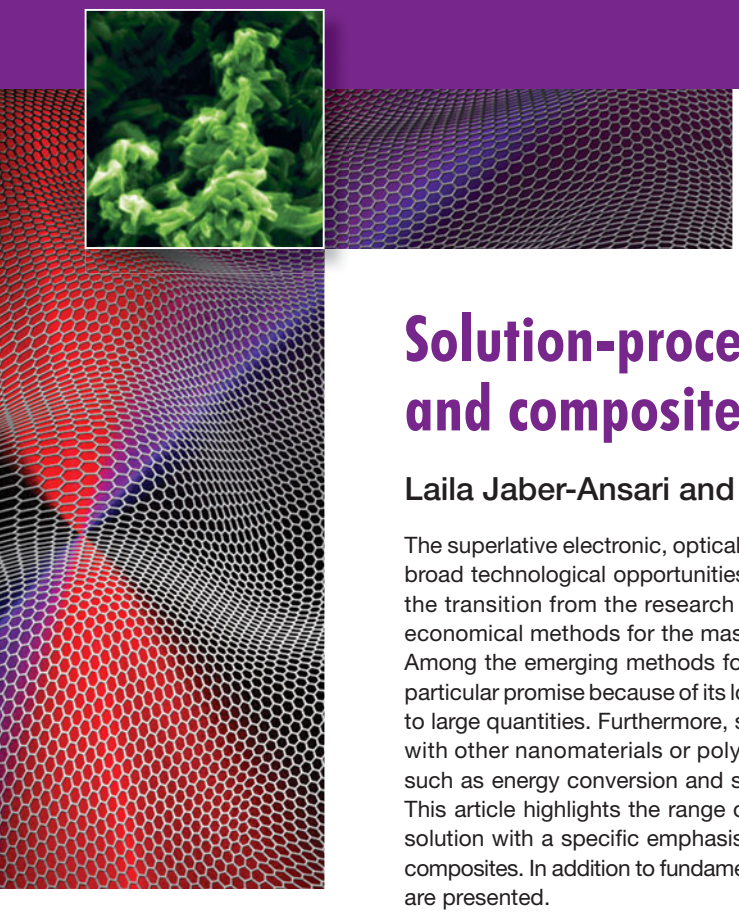


Solution-processed graphene materials and composites

Laila Jaber-Ansari and Mark C. Hersam

The superlative electronic, optical, mechanical, and chemical properties of graphene suggest broad technological opportunities for graphene-based materials and composites. However, the transition from the research laboratory to widespread commercial utilization requires economical methods for the mass production of graphene and graphene-based materials. Among the emerging methods for synthesizing graphene, solution-based processing holds particular promise because of its low cost, high throughput, chemical versatility, and scalability to large quantities. Furthermore, solution-processed graphene can be seamlessly integrated with other nanomaterials or polymers to yield composites for a wide array of applications such as energy conversion and storage, catalysis, electronics, and high-strength materials. This article highlights the range of techniques being developed for processing graphene in solution with a specific emphasis on solution-based methods for realizing graphene-based composites. In addition to fundamental principles, representative applications for these materials are presented.

Introduction

Graphene achieved widespread attention when it was separated from graphite in 2004 using the micromechanical exfoliation (i.e., adhesive tape) method.[1] Although micromechanical exfoliation is a straightforward and easily reproduced method that results in high-quality graphene suitable for fundamental studies, it lacks sufficient scalability for the bulk production of graphene-based materials. Similarly, chemical vapor deposition (CVD) of graphene on metal substrates and epitaxial growth of graphene on silicon carbide (see the articles by Nyakiti et al. and Bartelt and McCarty in this issue) are well-suited for planar applications (e.g., integrated circuits), but are not naturally extended to three-dimensional graphene-based composites.[2–4] In contrast, solution methods for isolating graphene exhibit several attributes that overcome the limitations of micromechanical exfoliation and high-temperature growth techniques, including (1) utilization of inexpensive graphite powder as the source material, (2) elimination of the need to transfer graphene from the growth substrate, (3) scalability to large-volume processing for industrial applications, and (4) amenability to mixing with polymers or other nanomaterials to form graphene nanocomposites.

In this article, we review solution processing of graphene with a particular focus on methods that enable the incorporation of graphene and related materials into bulk materials and composites. For organizational purposes, the solution-processing methods are separated into four major categories: (1) oxidation and subsequent reduction of graphite as a pathway to isolating graphene oxide and reduced graphene oxide, respectively; (2) exfoliation of graphene in aqueous solutions using amphiphilic surfactants; (3) direct exfoliation of graphene in organic solvents; and (4) exfoliation of graphene using intercalation and electrochemical methods. After describing these solution-based methods, we outline the integration of graphene with polymers and other nanomaterials in bulk material and nanocomposite forms. Furthermore, representative applications in energy conversion and storage, catalysis, electronics, and high-strength materials are delineated throughout the article in an effort to foreshadow the expected technological impact of graphene-based materials and composites.

Isolating graphene through solution processing

Synthesis and characterization of graphene oxide and reduced graphene oxide

Oxidation of graphite to graphite oxide (now commonly called graphene oxide [GO]) traces its origins to 1859, when Brodie used fuming nitric acid and potassium chlorate ($KClO_3$) to oxidize graphite.[5] Approximately a century later, Hummers and Offeman developed a procedure for oxidizing graphite that used potassium permanganate ($KMnO_4$) and sulfuric

Laila Jaber-Ansari, Materials Science and Engineering, Northwestern University; lailajaber2013@u.northwestern.edu
Mark C. Hersam, Materials Science and Engineering, Northwestern University; m-hersam@northwestern.edu
DOI: 10.1557/mrs.2012.182

© 2012 Materials Research Society

https://doi.org/10.1557/mrs.2012.182 Published online by Cambridge University Press

acid as oxidative agents.[6] Following this pioneering work, the Hummers method and its variants[7] have been widely used for GO formation.[7–12]

Nuclear magnetic resonance (NMR) and infrared (IR) spectroscopies and x-ray diffraction (XRD) indicate that hydroxyl and carbonyl groups decorate the surface of GO formed by these oxidation methods (**Figure 1**a). These hydroxyl and carbonyl groups provide electrostatic repulsion between GO sheets, thus minimizing aggregation in solution.[13,16–18] Furthermore, these oxygen moieties render GO hydrophilic, which enables straightforward dispersion in aqueous solution through sonication.[19,20] Once in solution, the dispersed graphene oxide sheets can then be converted to reduced graphene oxide (RGO) through chemical reduction, as schematically depicted in Figure 1b.[14] Figure 1c shows an atomic force microscopy image of GO sheets produced by a modified Hummers method. The GO sheets have an average lateral size of about 1 μm and a thickness of approximately 1 nm.[13]

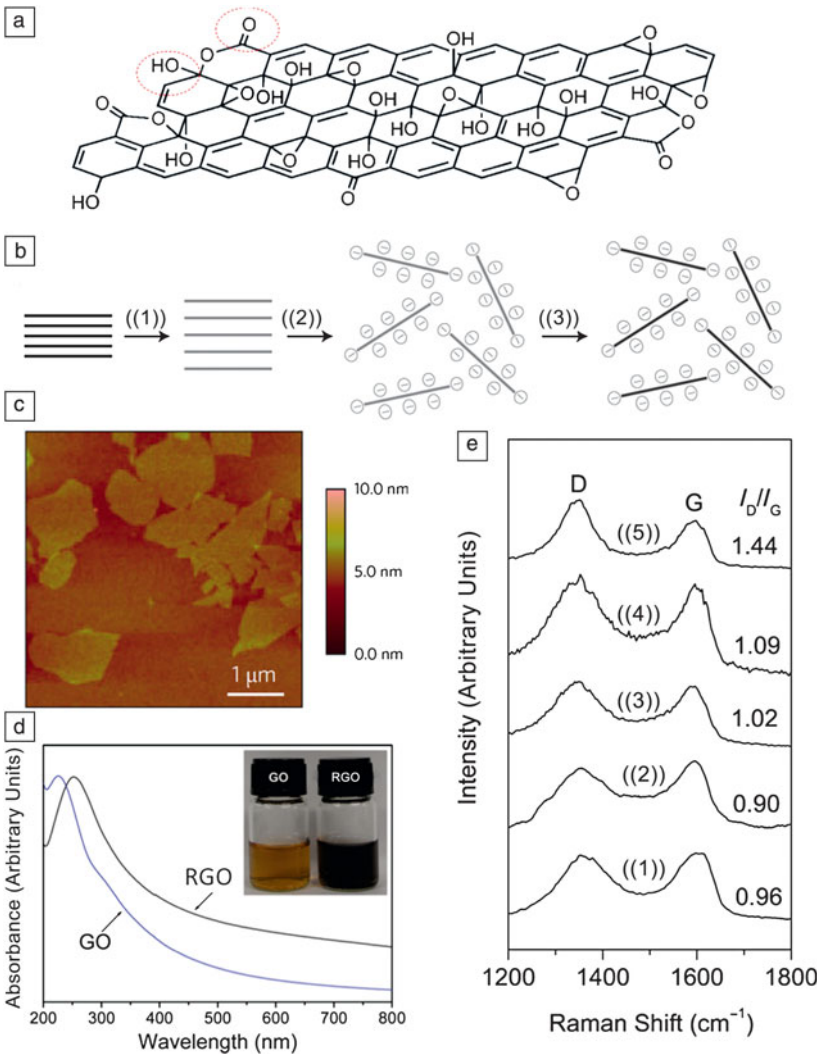


Figure 1. (a) Structural model of graphene oxide (GO) showing hydroxyl and carbonyl groups. Adapted from Reference 13. (b) Schematic illustration of the synthesis of aqueous graphene dispersions: ((1)) oxidation of graphite (black blocks) to graphite oxide (light gray blocks) with greater interlayer distance, ((2)) exfoliation of GO in water by sonication to obtain GO colloids, and ((3)) chemical conversion of GO to RGO in solution. Reproduced with permission from Reference 14. ©2008, Nature Publishing Group. (c) Atomic force microscopy image of GO sheets on a silicon substrate. Reproduced with permission from Reference 13. ©2009, Nature Publishing Group. (d) Optical absorbance spectra of GO and RGO. (e) Raman spectra of ((1)) GO; RGO obtained by hydrothermal treatment of GO at ((2)) 180°C, ((3)) 150°C, and ((4)) 120°C for 6 h; and ((5)) hydrazine-reduced GO, indicating the increased intensity of defect peaks (I_D) relative to graphene peaks (I_G) for chemically and hydrothermally reduced GO compared to GO. Parts (d) and (e) reproduced with permission from Reference 15. ©2009, American Chemical Society.

Several applications have been demonstrated for GO prepared by the Hummers method. For example, as-produced GO has been used as a catalyst in reactions such as oxidation of alcohols and alkyls,[21] as a surfactant to disperse other nanomaterials such as carbon nanotubes (CNTs) in aqueous solution,[22] and as a hole-transport and electron-blocking layer in organic photovoltaics.[23,24] Furthermore, GO exhibits intrinsic and tunable fluorescence, indicating potential application as an optical material.[25]

More commonly, however, GO serves as a precursor to RGO. The reduction of GO has been achieved chemically with reducing agents such as hydrazine,[14,26–28] zinc powder,[29] iron powder,[8] dimethylformamide (DMF),[30] laser irradiation,[31] poly(diallyldimethylammonium chloride) (PDDA),[32] and nontoxic reducing agents such as green tea[33] and vitamin C.[34] Other GO reduction methods include simultaneous electrochemical reduction and deposition on surfaces[35] and high-temperature reduction of GO sheets in a reducing gas atmosphere such as hydrogen. The latter approach is often used for synthesizing RGO composites, papers, or thin films for electronics and energy applications.[36,37]

As illustrated in Figure 1d, GO colloidal suspensions undergo a color change from yellow to black when RGO is formed.[15] RGO has been employed in many applications, including transistors and transparent conductors,[38–45] biological and chemical sensors,[35,46–48] and photovoltaics.[49,50] In comparison with mechanically exfoliated graphene, RGO exhibits more topological defects and a higher surface roughness.[51] Figure 1e shows the defect (D) peaks in the Raman spectra of chemically and hydrothermally reduced GO.[15] As a result of these defects and remnant oxygen functionalities, the electrical properties of RGO are compromised compared to those of pristine graphene.[52]

Exfoliation of graphite in aqueous solutions with amphiphilic surfactants

In an effort to avoid the defects introduced during the aforementioned oxidative and

https://doi.org/10.1557/mrs.2012.182 Published online by Cambridge University Press

reductive chemical treatments, researchers have also developed methods for directly exfoliating graphene from graphite in aqueous solutions using ultrasonication in amphiphilic surfactants such as sodium dodecyl benzene sulfonate (SDBS),[53] sodium cholate (SC), and sodium dodecyl sulfate (SDS).[54] Biocompatible, amphiphilic block copolymers (such as those sold under the trade names Pluronic and Tetronic) have also yielded effective dispersion of graphene in aqueous solutions.[55] These block copolymers contain hydrophobic poly(propylene oxide) (PPO) and hydrophilic poly(ethylene oxide) (PEO) domains that preferentially interact with graphene sheets and water molecules, respectively, enabling the graphene sheets to disperse in water without a covalent modification step. The concentration of graphene in aqueous solution depends on the lengths of the PPO and PEO chains, as shown in **Figure 2**a.[55]

Figure 2b schematically illustrates the ultrasonic exfoliation of graphene from graphite in aqueous solution containing SC.[54] As indicated in the schematic, solution-phase methods for directly exfoliating graphene from graphite typically offer minimal control over the thickness (i.e., number of layers) in the dispersed graphene sheets, which is suboptimal for many applications because many properties of graphene depend on the number of layers.[56] For example, single-layer graphene is a zero-bandgap semimetal,[57] whereas bilayer graphene has a tunable bandgap in the infrared region[58] and trilayer graphene has a band overlap that can be controlled by applying an electric field.[59]

An important advantage of dispersing graphene in aqueous solutions is that these solutions are compatible with methods for separating and purifying nanomaterials such as density-gradient ultracentrifugation (DGU).[60,61] For example, SC has a planar structure and can encapsulate few-layer-graphene particles to form well-ordered graphene/SC assemblies (as illustrated in Figure 2b). With this geometry, the buoyant density of these graphene/SC particles varies as a function of their thickness, presenting an opportunity for thickness sorting by DGU. In the graphene DGU process, SC-coated graphene sheets are initially loaded into a fluid of linearly varying density. During subsequent ultracentrifugation, the graphene sheets sediment through the density gradient until they reach the point where their density matches the local density of the fluid, forming distinct bands in the centrifuge tube. These bands contain graphene sheets with specific numbers of layers, which are then harvested in a fractionation step. Figure 2c shows these bands in a centrifuge tube along with atomic force microscopy characterization of selected fractions, illustrating separation by graphene thickness and thus number of layers.[54] Single-layer graphene isolated by DGU was recently employed in high-performance flexible electronic devices that operate at frequencies in the gigahertz range.[62]

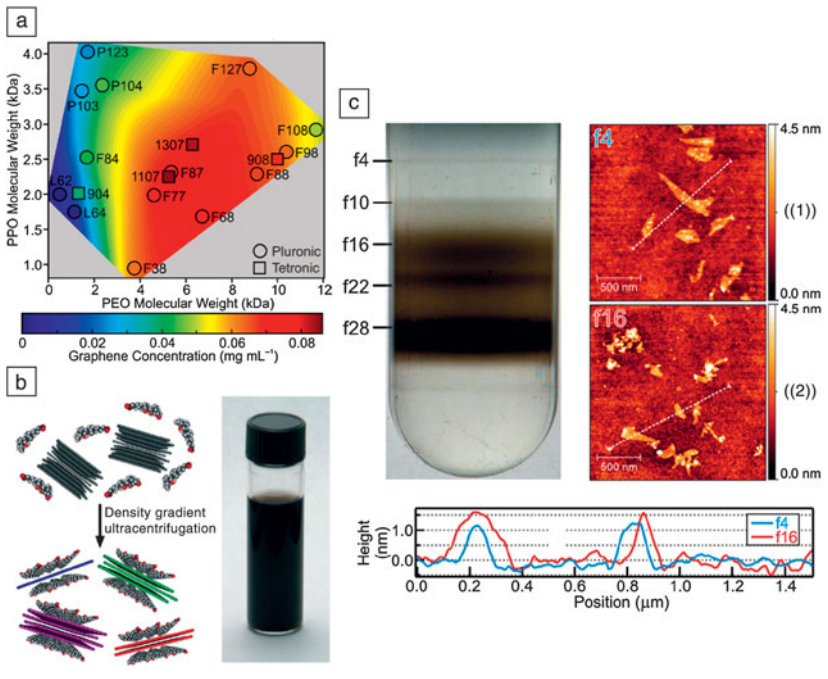


Figure 2. (a) Graphene concentration map for various Pluronic and Tetronic compositions (identified by trade name), showing the dependence of the concentration of graphene in aqueous solution on the lengths of the poly(propylene oxide) (PPO) and poly(ethylene oxide) (PEO) blocks of the block copolymers. Reproduced with permission from Reference 55. ©2011, American Chemical Society. (b) Schematic illustration of a surfactant-based graphene exfoliation process in aqueous solution, along with a photograph of a 90 μg ml^{-1} graphene dispersion in sodium cholate (SC). (c) Photograph of a centrifuge tube containing an aqueous solution of SC-coated graphene after the application of density gradient ultracentrifugation (DGU) and representative atomic force microscopy images of graphene from fractions designated ((1)) f4 and ((2)) f16 on a SiO_2 substrate. The height profiles corresponding to the indicated line scans from the two fractions demonstrate the different thicknesses of graphene flakes, in this case about 1 nm and 1.5 nm, segregated using DGU. Parts (b) and (c) reproduced with permission from Reference 54. ©2009, American Chemical Society.

Direct exfoliation of graphene in organic solvents

Another effective solution-phase method for exfoliating graphene from graphite is sonication of pristine graphite in organic solvents.[63–65] For example, Hernandez et al. used organic solvents such as *N*-methyl-2-pyrrolidone (NMP), γ-butyrolactone (GBL), *N*,*N*-dimethylacetamide (DMA), and *N*,*N*′-dimethylethyleneurea (DMEU) to obtain graphene dispersions with ~1 wt% yield (although the yield could be increased to ~12 wt% by recycling the graphite sediment). Because a mild-bath sonication was used for graphite exfoliation followed by a gentle centrifugation step for sedimentation and separation of the remaining graphite, the resulting graphene was reported to have a low defect density as determined by Raman spectroscopy.[63] With this method, graphene dispersions with concentrations of approximately

https://doi.org/10.1557/mrs.2012.182 Published online by Cambridge University Press

0.01 mg/ml were obtained in various solvents. **Figure 3**a–b show the optical absorbance data for such solutions. NMP was found to be the best choice among the four tested solvents for graphene exfoliation, yielding the highest graphene concentration, because its surface energy provides the best match with the surface energy of graphene.[63]

For applications that require higher graphene concentrations, Liang et al. employed a stabilizer and solvent-exchange method to increase the concentration of graphene in organic solvents. They initially used ethanol as a solvent to exfoliate graphite and obtained a graphene dispersion with a concentration of 1.6 μg/ml. However, upon addition of ~1% w/v ethyl cellulose (EC) to ethanol, the graphene concentration was substantially enhanced to more than 120 μg/ml. Terpineol was then added to dilute this solution to about 100 μg/ml. Because the EC-stabilized graphene flakes are hydrophobic, subsequent addition of water to the graphene/terpineol/ethanol/EC solution induced the graphene to leave the EC phase and concentrate in the small-volume terpineol phase, resulting in a graphene ink with a concentration of about 1 mg/ml following three iterations of this solvent-exchange process (Figure 3c).[66]

Exfoliation of graphene using intercalation and electrochemical methods

Graphite intercalation compounds such as tetrabutylammonium hydroxide (TBA) have also been used for exfoliation of graphite or weakly oxidized graphite oxide. Although this method yields large graphene flakes, the resulting graphene contains significant quantities of defects.[67,68] Ionic intercalation compounds can also be used for graphite exfoliation, but they either leave oxygen moieties on the graphene sheets or produce graphene flakes that are relatively small compared to those obtained using competing intercalation compounds (e.g., TBA).[69,70]

To address these issues, Shih et al. used halides (ICl and IBr) as intercalants for graphite.[71] In this method, a piece of highly oriented pyrolytic graphite (HOPG) was placed in a reactor along with the intercalation compounds and heated to 100–160°C for 48 h. The intercalated graphite was then immediately heated to 800°C in an argon atmosphere, leading to volumetric expansion. The degree of intercalation is controlled by the intercalation temperature, providing significant tunability. For example, every third layer of the graphite lattice can be intercalated (stage 3), or every second layer can be intercalated (stage 2), as shown in **Figure 4**a. These well-ordered crystallographic stages are demonstrated by the XRD patterns in Figure 4b.

Stage-2 and stage-3 expanded samples exhibit a substantial volume expansion, as shown in Figure 4c–d. The two bottom profiles in Figure 4b show the XRD patterns of stage-2 and stage-3 expanded graphite. The corresponding (002) and (004) peak positions are almost identical to those of HOPG, indicating that the spacing of the graphene planes in graphite is restored. Furthermore, the decrease in (004) peak intensity and the absence of the (006) peak show that the two materials are made of fewer than four graphite layers.[71]

Inspired by electrochemical reactions in lithium-ion batteries, Wang et al. used intercalation of lithium ions in graphite to exfoliate graphite. The primary advantage of this method is the high yield of single- and few-layer graphene (more than 70%), whereas the yield is often less than 1% in competing exfoliation methods. In the lithium intercalation process, graphite is used as the negative electrode in a lithium-ion battery cell.[72] In many commercial lithium-ion batteries, electrolytes are selected so that they form a protective layer on the graphite anode that is referred to as the solid electrolyte interphase (SEI). SEI formation prevents graphite exfoliation and promotes a longer battery life.[73] Therefore, for effective graphite exfoliation with the highest yield, electrolytes are needed that do not form an SEI layer, such as propylene carbonate (PC).[74] To further promote exfoliation, Wang et al. used a high applied potential (–15 ± 5 V) to activate the intercalation of PC molecules in addition to Li^+ ions into the graphite.[72] The resulting expanded graphite was then exfoliated to graphene by sonication in LiCl in a DMF/PC mixed solvent. Figure 4e schematically illustrates this process.[72]

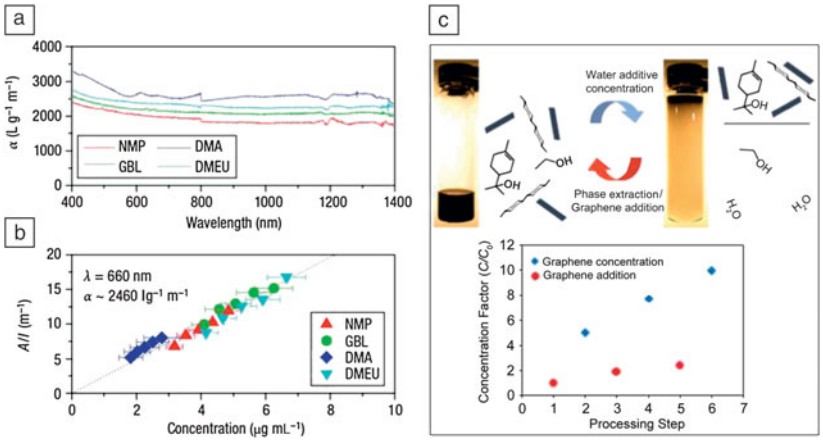


Figure 3. (a) Absorption spectra for few-layer graphene dispersed in *N*-methyl-2-pyrrolidone (NMP), γ-butyrolactone (GBL), *N*,*N*-dimethylacetamide (DMA), and *N*,*N*′-dimethylethyleneurea (DMEU) at concentrations from 2 to 8 μg ml^{-1}. (b) Optical absorbance, *A* (at λ = 660 nm), divided by cell length (*l*) for graphene in the four solvents NMP, GBL, DMA, and DMEU, showing Beer–Lambert behavior (absorbance proportional to concentration and path length) with an average absorption coefficient of $\langle\alpha_{660}\rangle \approx 2460$ l g^{-1} m^{-1}. The *x*-axis error bars indicate the uncertainty in measuring the mass of graphene/graphite in solution. Parts (a) and (b) reproduced with permission from Reference 63. ©2008, Nature Publishing Group. (c) Vials of a 1:5 mixture of terpineol and ethyl cellulose stabilized graphene/ethanol solution before and after water addition. Upon the addition of water, the hydrophobic graphene flakes preferentially separate into the concentrated terpineol fraction, leaving behind a predominantly ethanol and water mixture. The concentration factor C/C_0 of graphene (for an initial concentration of C_0 = 102.4 μg/ml) is plotted after each solvent-exchange concentration and graphene/ethanol addition step for three iterations. Reproduced with permission from Reference 66. ©2010, American Chemical Society.

https://doi.org/10.1557/mrs.2012.182 Published online by Cambridge University Press

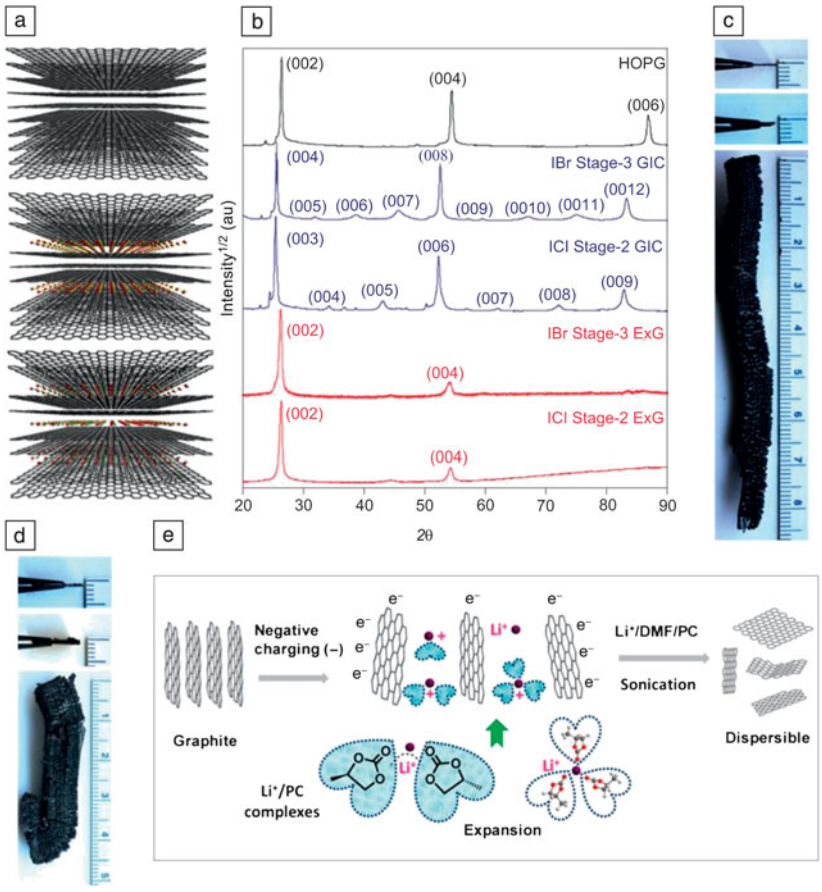


Figure 4. (a) Schematic illustration of highly oriented pyrolytic graphite (HOPG) (top), IBr stage-3 graphite intercalation compound (GIC) (middle), and ICl stage-2 GIC (bottom) (carbon, gray; iodine, red; bromine, yellow; chlorine, cyan). (b) X-ray diffraction patterns of HOPG, IBr stage-3 GIC, ICl stage-2 GIC, IBr stage-3 expanded graphite (ExG), and ICl stage-2 ExG. For IBr stage-3 GIC, three additional peaks appear between two of the three main peaks corresponding to the (002), (004), and (006) planes in HOPG, which is a clear signature of stage-3 GIC (the intercalant layer inserts between every three graphene layers). (c) Photographs of HOPG (top), stage-3 GIC (middle), and stage-3 ExG formed by lithium intercalation (bottom). (The HOPG and GIC materials are held up with tweezers with the edges toward the viewer). (d) Photographs of HOPG (top), stage-2 GIC (middle), and stage-2 ExG (bottom). Parts (a)–(d) reproduced with permission from Reference 71. ©2011, Nature Publishing Group. (e) Schematic illustration of electrochemically charged graphite in Li$^+$/propylene carbonate (PC). The expanded graphite is then exfoliated by power sonication in LiCl in a dimethylformamide/PC mixed solvent. Part (e) reproduced with permission from Reference 72. ©2011, American Chemical Society.

Amphiphilic surfactants such as SDS have also been used as intercalating compounds. In addition to serving as intercalants, the surfactants that adsorb on the surface of the exfoliated graphene sheets prevent the sheets from restacking in solution following exfoliation. In this method, a graphite rod is used as a working electrode with a platinum counter electrode in a 1% SDS aqueous solution. The graphite rod is initially treated as an anode in an effort to drive SDS intercalation. Then, the intercalated graphite is treated as a cathode, leading to the exfoliation and dispersion of SDS-functionalized graphene sheets. The size and concentration of the graphene sheets can be controlled by the intercalation potential, thus providing a degree of dispersion tunability.[75]

Solution-processed graphene composites

Because of its extended sp^2-hybridized carbon network, graphene has exceptional electrical and thermal conductivity and superlative mechanical properties, thus making it a promising candidate for composite materials.[76,77] Additive components that are commonly used for synthesizing graphene composites are polymers and nanoparticles of metals, metal compounds, and carbon. Solution-processing methods such as solution mixing and *in situ* polymerization have the advantage of producing well-mixed composites in comparison with other methods such as melt compounding. The following two subsections provide representative examples of graphene/polymer and graphene/nanoparticle composites.

Graphene/polymer composites

Graphene, GO, and RGO composites with insulating and conducting polymers have been widely reported in the literature.[78–91] In the solution-mixing method for synthesizing graphene/polymer composites, a graphene, GO, or RGO colloidal dispersion is combined with the polymer in solution. This approach has been employed with a variety of both nonconducting polymers such as poly(vinyl alcohol),[83,88,92] poly(methyl methacrylate),[92] poly(vinylidene fluoride),[93] polystyrene,[94,95] and polycarbonate[96] and conducting polymers such as sulfonated poly(phenylene ethylene),[84] poly(3-hexylthiophene-2,5-diyl),[97] and poly (3,4-ethylenedioxythiophene).[98] **Figure 5** provides an example of the processing and resulting structure of a representative graphene/polymer composite.

In polymer composites that contain RGO, reduction of graphene oxide to RGO can be performed either before or after solution mixing. In the pregraphitization strategy, RGO is directly mixed with the polymer, thus avoiding exposure of the polymer to the graphene oxide reduction process that involves chemical treatments or high temperatures. On the other hand, the advantage of the postgraphitization strategy is that GO is easily dispersed in aqueous solutions because of its hydrophilicity, thus enabling the integration of GO with water-soluble polymers using a simple sonication step. Unfunctionalized graphene sheets that do not disperse well in water can be dispersed in solvents such as DMF[99] and then mixed with the polymer solution. After the solutions are mixed, the composite can be precipitated by water/solvent evaporation,[100] filtration,[101] centrifugation,[102] or flocculation (for example, adding alcohol to a water-dispersed composite causes composite precipitation).[103]

https://doi.org/10.1557/mrs.2012.182 Published online by Cambridge University Press

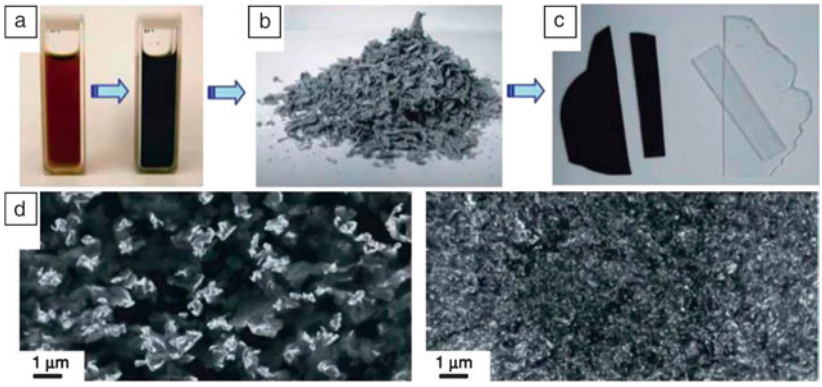


Figure 5. An example of a fabrication process for a graphene/polymer composite: (a) Suspension of phenyl isocyanate-treated GO (1 mg/ml) and dissolved polystyrene in dimethylformamide before (left) and after (right) reduction of the GO by *N*,*N*-dimethylhydrazine. (b) Composite powder as obtained after coagulation in methanol. (c) Hot-pressed composite (opaque; 0.12 vol% graphene) and pure polystyrene (clear) of the same 0.4-mm thickness following identical processing. (d) Scanning electron microscopy (SEM) images obtained from a fracture surface of composite samples of 0.48 vol% (left) and 2.4 vol% (right) graphene in polystyrene. Reproduced with permission from Reference 94. ©2006, Nature Publishing Group.

In situ polymerization is another common solution method for synthesizing graphene/polymer composites. In this method, the monomer is mixed with the graphene, GO, or RGO colloidal suspension, and then polymerization is induced. Both pre- and postgraphitization processes are compatible with this strategy.[104,105] As an example, Hu et al. prepared graphene/polystyrene nanocomposites by mixing GO with styrene monomers and then inducing polymerization by adding potassium persulfate and heating in an inert atmosphere. In this case, hydrazine was then added to induce GO reduction to RGO.[105] This method tends to promote uniform coating of the graphene within the polymer matrix. However, the disadvantage is that interchain hydrogen bonding can be inhibited, resulting in a slight degradation in mechanical properties.[106]

Applications for graphene-based polymer composites attempt to exploit the unique electrical, physical, and chemical properties of graphene and graphene oxide. For example, because of their high conductivities, polymer composites of graphene and RGO have been used in field-effect transistors,[107] supercapacitors,[101] and photovoltaics.[50,108] Other applications such as biosensors[109,110] and biomedical[111] applications rely on the high mechanical strength of graphene and GO[112,113] and the chemical stability of graphene. **Figure 6**a–b show scanning electron microscopy (SEM) and transmission electron microscopy (TEM) images of a composite of graphene nanosheets (GNSs) and polyaniline (PANI). PANI is generally regarded as a promising electrode material for supercapacitors because of its high energy-storage capacity. Figure 6c shows that addition of graphene nanosheets to PANI further improves this capacity by increasing the available surface area and conductivity of the PANI electrode.[101]

Graphene/nanoparticle composites

Graphene and GO composites with other carbonaceous nanomaterials such as fullerenes and CNTs have also been reported.[114–117] Typically, a colloidal dispersion of graphene or GO is directly mixed with another carbon nanomaterial dispersion and sonicated to form a uniform dispersion. The composite is then formed by vacuum filtration, drop casting, or blade coating of the mixed solution. In some cases, GO acts as a surfactant for the dispersion of CNTs in aqueous solutions because of its amphiphilic nature (GO has hydrophilic edges and hydrophobic regions on its basal plane).[22] The addition of CNTs and fullerenes can increase the conductivity of graphene-based materials, which has utility for applications in electronics and transparent conductors.[117]

Metal and metal-compound nanoparticles have also been explored as additives in graphene-based composites.[118–130] As for carbon-based nanomaterials, the most common method for preparing these composites is solution mixing of dispersions of graphene and a metal or metal compound. In addition, *in situ* methods for directly depositing nanoparticles on graphene sheets in solution have been reported.[131–134] For example, HongKun and Chao demonstrated that gold, platinum, palladium, and silver nanoparticles can be deposited on RGO from their precursors

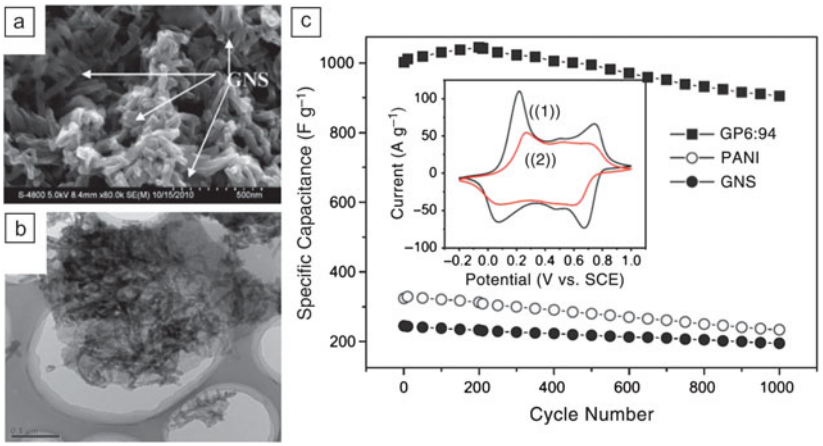


Figure 6. (a) SEM and (b) transmission electron microscopy (TEM) images of a polyaniline (PANI)/graphene composite. (c) Variation of the specific capacitance of pure PANI, graphene nanosheets (GNSs), and graphene/polymer (GP) (6:94) composite electrodes as a function of cycle number measured at a rate of 50 mV s^{-1} in 1 M H_2SO_4 aqueous solution. The inset shows the ((1)) first and ((2)) 1000th cyclic voltammograms of the GP6:94 composite. Reproduced with permission from Reference 101. ©2011, Elsevier.

https://doi.org/10.1557/mrs.2012.182 Published online by Cambridge University Press

($AuCl_3$·HCl·H_2O, K_2PtCl_4, $PdCl_2$, and $AgNO_3$, respectively). These composites exhibited enhanced catalytic activity for the reduction reaction of potassium hexacyanoferrate(III).[134] Yang et al. also reported enhancement in electrocatalytic activity of graphene following decoration with gold nanoparticles, with potential applications in biomedical and energy technologies.[131] Similarly, RGO/silver nanoparticle composites showed excellent antibacterial capability comparable to that of the antibacterial drug ampicillin,[128] whereas graphene/iron nanoparticle[135] and graphene/tin nanoparticle[136] composites were reported to have high lithium-ion capacities for use in rechargeable lithium-ion batteries.

A variety of metal compounds have also been employed in graphene/nanoparticle composites. For instance, graphene and RGO have been incorporated into composites with Fe_3O_4,[124] vanadium nitride,[137] MnO_2,[138,139] Mn_3O_4,[140] SnO_2,[125,141] MoO_2,[139] TiO_2,[142] and CuO[143] for application in high-performance lithium-ion battery electrodes. In addition, RGO composites with CdS[118] and ZnO[144] were used for photocatalytic reduction of Cr(VI), and RGO composites with MnO_2 were utilized in supercapacitors.[138] **Figure 7**a–b show TEM and high-resolution TEM images, respectively, of an RGO/Mn_3O_4 composite. Figure 7c–d compare the specific lithium capacity and battery cycling performance of pure Mn_3O_4 and RGO/Mn_3O_4 composite, respectively, revealing improvement in the reversible capacity following the addition of RGO.[140] Figure 7e–f show SEM images of solvent-exfoliated graphene (SEG) and solvent-reduced graphene oxide (SRGO) composites with mixed-phase titania (TiO_2 P25) particles. These composites act as effective catalysts for CH_3CHO photo-oxidation and CO_2 photoreduction reactions, respectively. In particular, SEG-based composites were found to exhibit higher catalytic activity than SRGO-based composites in both oxidation and reduction reactions. This observation was attributed to the reduced defect density and thus higher electron mean free path for SEG compared to SRGO.[145]

Conclusions and perspective

Solution-processing techniques have helped graphene-based research proliferate because they provide relatively straightforward access to large quantities of graphene, thus enabling widespread exploration of graphene materials and composites in fundamental studies and application development. Various solution methods have emerged for scalable exfoliation of graphite to graphene, including aqueous surfactant, solvent, and electrochemical exfoliation of graphene in addition to oxidation/reduction graphene oxide/reduced graphene oxide pathways. Because each of these methods involves tradeoffs in the quality and size of graphene sheets, processing time, and yield, the choice of graphene dispersion method is often dictated by the needs of the specific experiment or application. After being dispersed in the solution phase, graphene can be straightforwardly integrated with a variety of polymer and/or nanomaterial solutions, providing vast opportunities for the synthesis and testing of graphene-based composites. These composites are already impacting numerous applications, including electronics, biomedical devices, and energy conversion and storage technologies.

Despite the rapid progress and many accomplishments in this field, important challenges remain for solution-processed

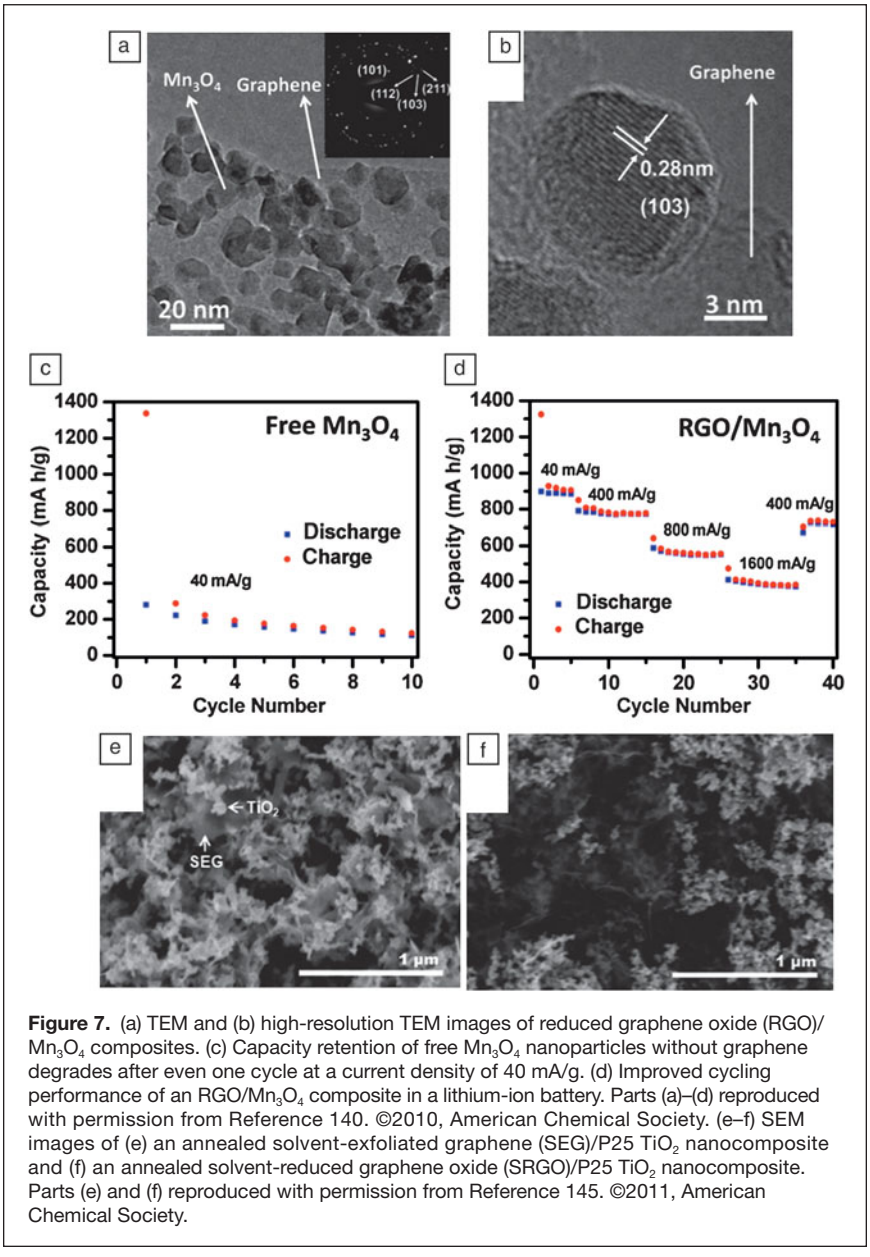


Figure 7. (a) TEM and (b) high-resolution TEM images of reduced graphene oxide (RGO)/Mn_3O_4 composites. (c) Capacity retention of free Mn_3O_4 nanoparticles without graphene degrades after even one cycle at a current density of 40 mA/g. (d) Improved cycling performance of an RGO/Mn_3O_4 composite in a lithium-ion battery. Parts (a)–(d) reproduced with permission from Reference 140. ©2010, American Chemical Society. (e–f) SEM images of (e) an annealed solvent-exfoliated graphene (SEG)/P25 TiO_2 nanocomposite and (f) an annealed solvent-reduced graphene oxide (SRGO)/P25 TiO_2 nanocomposite. Parts (e) and (f) reproduced with permission from Reference 145. ©2011, American Chemical Society.

https://doi.org/10.1557/mrs.2012.182 Published online by Cambridge University Press

graphene. Because many graphene properties depend on the size and number of graphene layers, methods for better control of the monodispersity of these parameters are needed. In addition, solution-phase processing techniques typically yield graphene flakes with relatively small lateral sizes (less than 100 μm^2) despite the advantages that larger flakes have in high-performance applications (e.g., electronics). Methods for directly controlling or postsynthetically selecting the number of graphene layers also remain of high interest. In this regard, intercalation methods[71] show promise and will likely be the subject of future efforts in this field.

Another emerging challenge is the direct solution-phase exfoliation or synthesis of graphene nanoribbons[146,147] with tunable widths, which are of interest because of their potential applicability in digital electronics. Similarly, biomedical applications of graphene[148,149] are in their infancy but are expected to expand as methods emerge to improve the biocompatibility of graphene dispersions.[150] Finally, practical issues including throughput, yield, and cost will require continual attention and innovation as graphene materials and composites transition from research laboratories to nascent industrial-scale applications.

Acknowledgments

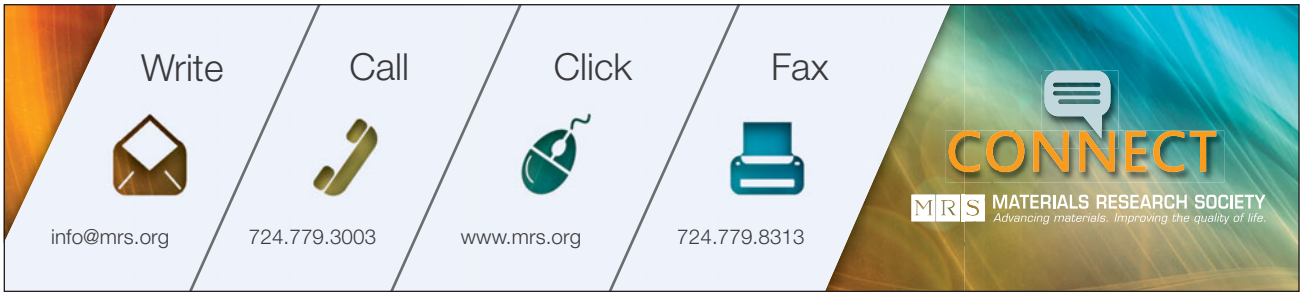
This work was supported by the Center for Electrical Energy Storage, an Energy Frontier Research Center funded by the US Department of Energy, Office of Science, Office of Basic Energy Sciences (Award DE-AC02-06CH11357).

References

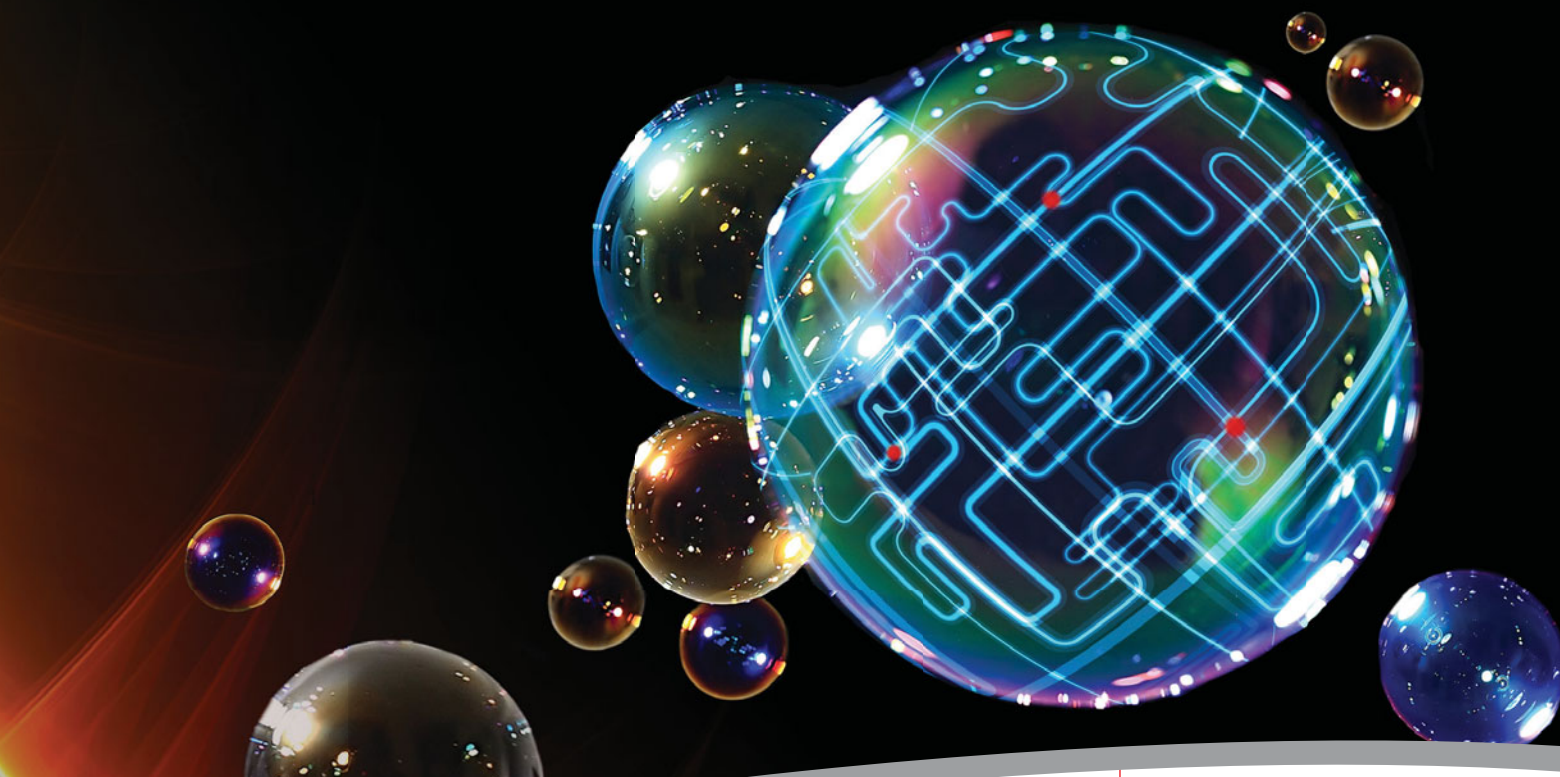
1. K.S. Novoselov, K.A. Geim, S.V. Morozov, D. Jiang, Y. Zhang, S.V. Dubonos, I.V. Grigorieva, A.A. Firsov, *Science* **306**, 666 (2004).
2. J. Hass, W.A. de Heer, E.H. Conrad, *J. Phys.: Condens. Matter* **20**, 323202 (2008).
3. A. Reina, X. Jia, J. Ho, D. Nezich, H. Son, V. Bulovic, M.S. Dresselhaus, J. Kong, *Nano Lett.* **9**, 30 (2009).
4. X. Li, W. Cai, J. An, S. Kim, J. Nah, D. Yang, R. Piner, A. Velamakanni, I. Jung, E. Tutuc, S.K. Banerjee, L. Colombo, R.S. Ruoff, *Science* **324**, 1312 (2009).
5. B.C. Brodie, *Philos. Trans. R. Soc. London* **149**, 249 (1859).
6. W.S. Hummers, R.E. Offeman, *J. Am. Chem. Soc.* **80**, 1339 (1958).
7. N.I. Kovtyukhova, P.J. Ollivier, B.R. Martin, T.E. Mallouk, S.A. Chizhik, E.V. Buzaneva, A.D. Gorchinskiy, *Chem. Mater.* **11**, 771 (1999).
8. Z.J. Fan, W. Kai, J. Yan, T. Wei, L.J. Zhi, J. Feng, Y.M. Ren, L.P. Song, F. Wei, *ACS Nano* **5**, 191 (2011).
9. Z. Xu, C. Gao, *ACS Nano* **5**, 2908 (2011).
10. J. Zhang, H. Yang, G. Shen, P. Cheng, J. Zhang, S. Guo, *Chem. Commun.* **46**, 1112 (2010).
11. X. Zhou, Z. Liu, *Chem. Commun.* **46**, 2611 (2010).
12. X. Sun, Z. Liu, K. Welsher, J.T. Robinson, A. Goodwin, S. Zaric, H. Dai, *Nano Res.* **1**, 203 (2008).
13. W. Gao, L.B. Alemany, L. Ci, P.M. Ajayan, *Nat. Chem.* **1**, 403 (2009).
14. D. Li, M.B. Müller, S. Gilje, R.B. Kaner, G.G. Wallace, *Nat. Nanotechnol.* **3**, 101 (2008).
15. Y. Zhou, Q. Bao, L.A.L. Tang, Y. Zhong, K.P. Loh, *Chem. Mater.* **21**, 2950 (2009).
16. K. Josepovits, Y. Sanakis, D. Petridis, I. De, *Chem. Mater.* **18**, 2740 (2006).
17. A. Lerf, H. He, M. Forster, J. Klinowski, *J. Phys. Chem. B* **102**, 4477 (1998).
18. M.A. Rodriguez, V.P.S. Jimenez, *Carbon* **24**, 163 (1986).
19. G. Wang, J. Yang, J. Park, X. Gou, B. Wang, H. Liu, J. Yao, *J. Phys. Chem. C* **112**, 8192 (2008).
20. S. Stankovich, D.A. Dikin, R.D. Piner, K.A. Kohlhaas, A. Kleinhammes, Y. Jia, Y. Wu, S.T. Nguyen, R.S. Ruoff, *Carbon* **45**, 1558 (2007).
21. J. Pyun, *Angew. Chem.* **50**, 46 (2011).
22. L.J. Cote, J. Kim, V.C. Tung, J. Luo, F. Kim, J. Huang, *Pure Appl. Chem.* **83**, 95 (2011).
23. S.S. Li, K.H. Tu, C.C. Lin, C.W. Chen, M. Chhowalla, *ACS Nano* **4**, 3169 (2010).
24. I.P. Murray, S.J. Lou, L.J. Cote, S. Loser, C.J. Kadleck, T. Xu, J.M. Szarko, B.S. Rolczynski, J.E. Johns, J. Huang, L. Yu, L.X. Chen, T.J. Marks, M.C. Hersam, *J. Phys. Chem. Lett.* **2**, 3006 (2011).
25. K.P. Loh, Q. Bao, G. Eda, M. Chhowalla, *Nat. Chem.* **2**, 1015 (2010).
26. J. Yan, Z. Zhao, L. Pan, *Phys. Status Solidi A* **208**, 2335 (2011).
27. J. Long, M. Fang, G. Chen, *J. Mater. Chem.* **21**, 10421 (2011).
28. Y. Xu, H. Bai, G. Lu, C. Li, G. Shi, *J. Am. Chem. Soc.* **130**, 5856 (2008).
29. X. Mei, J. Ouyang, *Carbon* **49**, 5389 (2011).
30. K. Ai, Y. Liu, L. Lu, X. Cheng, L. Huo, *J. Mater. Chem.* **21**, 3365 (2011).
31. L. Huang, Y. Liu, L.C. Ji, Y.Q. Xie, T. Wang, W.Z. Shi, *Carbon* **49**, 2431 (2011).
32. S. Zhang, Y. Shao, H. Liao, M.H. Engelhard, G. Yin, Y. Lin, *ACS Nano* **5**, 1785 (2011).
33. Y. Wang, Z. Shi, J. Yin, *ACS Appl. Mater. Interfaces* **3**, 1127 (2011).
34. M.J. Fernandez-Merino, L. Guardia, J.I. Paredes, S. Villar-Rodil, P. Solis-Fernandez, A. Martinez-Alonso, J.M.D. Tascon, *J. Phys. Chem. C* **114**, 6426 (2010).
35. Y. Guo, B. Wu, H. Liu, Y. Ma, Y. Yang, J. Zheng, G. Yu, Y. Liu, *Adv. Mater.* **23**, 4626 (2011).
36. J.K. Lee, K.B. Smith, C.M. Hayner, H.H. Kung, *Chem. Commun.* **46**, 2025 (2010).
37. X. Wang, L. Zhi, K. Müllen, *Nano Lett.* **8**, 323 (2008).
38. B.J. Kim, V.H. Pham, T.V. Cuong, E.J. Kim, J.S. Chung, S.H. Hur, J.H. Cho, *J. Mater. Chem.* **21**, 13068 (2011).
39. J.M. Mativetsky, A. Liscio, E. Treossi, E. Orgiu, A. Zanelli, P. Samorì, V. Palermo, *J. Am. Chem. Soc.* **133**, 14320 (2011).
40. K. Suganuma, S. Watanabe, T. Gotou, K. Ueno, *Appl. Phys. Express* **4**, 021603 (2011).
41. Q. He, S. Wu, S. Gao, X. Cao, Z. Yin, H. Li, P. Chen, H. Zhang, *ACS Nano* **5**, 5038 (2011).
42. S. Wang, P.K. Ang, Z. Wang, A.L.L. Tang, J.T.L. Thong, K.P. Loh, *Nano Lett.* **10**, 92 (2010).
43. S. Pang, H.N. Tsao, X. Feng, K. Müllen, *Adv. Mater.* **21**, 3488 (2009).
44. G. Eda, G. Fanchini, M. Chhowalla, *Nat. Nanotechnol.* **3**, 270 (2008).
45. H.A. Becerril, J. Mao, Z. Liu, R.M. Stoltenberg, Z. Bao, Y. Chen, *ACS Nano* **2**, 463 (2008).
46. H. Jiang, *Small* **7**, 2413 (2011).
47. F. Li, J. Chai, H. Yang, D. Han, L. Niu, *Talanta* **81**, 1063 (2010).
48. Q. Ji, I. Honma, S.M. Paek, M. Akada, J.P. Hill, A. Vinu, K. Ariga, *Angew. Chem.* **49**, 9737 (2010).
49. Y. Xu, G. Long, L. Huang, Y. Huang, X. Wan, Y. Ma, Y. Chen, *Carbon* **48**, 3308 (2010).
50. Z. Liu, D. He, Y. Wang, H. Wu, J. Wang, *Sol. Energy Mater. Sol. Cells* **94**, 1196 (2010).
51. C. Gómez-Navarro, J.C. Meyer, R.S. Sundaram, A. Chuvilin, S. Kurasch, M. Burghard, K. Kern, U. Kaiser, *Nano Lett.* **10**, 1144 (2010).
52. V.C. Tung, M.J. Allen, Y. Yang, R.B. Kaner, *Nat. Nanotechnol.* **4**, 25 (2009).
53. M. Lotya, Y. Hernandez, P.J. King, R.J. Smith, V. Nicolosi, L.S. Karlsson, F.M. Blighe, S. De, Z. Wang, I.T. Mcgovern, G.S. Duesberg, J.N. Coleman, *J. Am. Chem. Soc.* **131**, 3611 (2009).
54. A.A. Green, M.C. Hersam, *Nano Lett.* **9**, 4031 (2009).
55. J.W.T. Seo, A.A. Green, A.L. Antaris, M.C. Hersam, *J. Phys. Chem. Lett.* **2**, 1004 (2011).
56. A.A. Green, M.C. Hersam, *J. Phys. Chem. Lett.* **1**, 544 (2010).
57. A. Castro Neto, F. Guinea, N. Peres, K. Novoselov, A. Geim, *Rev. Mod. Phys.* **81**, 109 (2009).
58. Y. Zhang, T.T. Tang, C. Girit, Z. Hao, M.C. Martin, A. Zettl, M.F. Crommie, Y.R. Shen, F. Wang, *Nature* **459**, 820 (2009).
59. M.F. Craciun, S. Russo, M. Yamamoto, J.B. Oostinga, A.F. Morpurgo, S. Tarucha, *Nat. Nanotechnol.* **4**, 383 (2009).
60. M.S. Arnold, A.A. Green, J.F. Hulvat, S.I. Stupp, M.C. Hersam, *Nat. Nanotechnol.* **1**, 60 (2006).
61. A.A. Green, M.C. Hersam, *Nat. Nanotechnol.* **4**, 64 (2009).
62. C. Sire, F. Ardiaca, S. Lepilliet, J.W.T. Seo, M.C. Hersam, G. Dambrine, H. Happy, V. Derycke, *Nano Lett.* **12**, 1184 (2012).
63. Y. Hernandez, V. Nicolosi, M. Lotya, F.M. Blighe, Z. Sun, S. De, I.T. McGovern, B. Holland, M. Byrne, Y.K. Gun'Ko, J.J. Boland, P. Niraj, G. Duesberg, S. Krishnamurthy, R. Goodhue, J. Hutchison, V. Scardaci, A.C. Ferrari, J.N. Coleman, *Nat. Nanotechnol.* **3**, 563 (2008).
64. Y.T. Liu, X.M. Xie, X.Y. Ye, *Carbon* **49**, 3529 (2011).
65. A. O'Neill, U. Khan, P.N. Nirmalraj, J. Boland, J.N. Coleman, *J. Phys. Chem. C* **115**, 5422 (2011).
66. Y.T. Liang, M.C. Hersam, *J. Am. Chem. Soc.* **132**, 17661 (2010).
67. P.K. Ang, S. Wang, Q. Bao, J.T.L. Thong, K.P. Loh, *ACS Nano* **3**, 3587 (2009).
68. X. Li, G. Zhang, X. Bai, X. Sun, X. Wang, E. Wang, H. Dai, *Nat. Nanotechnol.* **3**, 538 (2008).
69. J. Zheng, C.A. Di, Y. Liu, H. Liu, Y. Guo, C. Du, C.T. Wu, G. Yu, D. Zhu, *Chem. Commun.* **46**, 5728 (2010).

https://doi.org/10.1557/mrs.2012.182 Published online by Cambridge University Press

70. N. Behabtu, J.R. Lomeda, M.J. Green, A.L. Higginbotham, A. Sinitskii, D.V. Kosynkin, D. Tsentalovich, A.N.G. Parra-Vasquez, J. Schmidt, E. Kesselman, Y. Cohen, Y. Talmon, J.M. Tour, M. Pasquali, *Nat. Nanotechnol.* **5**, 406 (2010).
71. C.J. Shih, A. Vijayaraghavan, R. Krishnan, R. Sharma, J.H. Han, M.H. Ham, Z. Jin, S. Lin, G.L.C. Paulus, N.F. Reuel, Q.H. Wang, D. Blankschtein, M.S. Strano, *Nat. Nanotechnol.* **6**, 439 (2011).
72. J. Wang, K.K. Manga, Q. Bao, K.P. Loh, *J. Am. Chem. Soc.* **133**, 8888 (2011).
73. Z.X. Shu, R.S. Mcmillan, J.J. Murray, I.J. Davidson, *J. Am. Chem. Soc.* **43**, 2230 (1996).
74. R.D. Rauh, S.B. Brummer, *Electrochim. Acta* **22**, 75 (1977).
75. M. Alanyalıoğlu, J.J. Segura, J. Oró-Solè, N. Casañ-Pastor, *Carbon* **50**, 142 (2012).
76. A.A. Balandin, S. Ghosh, W. Bao, I. Calizo, D. Teweldebrhan, F. Miao, C.N. Lau, *Nano Lett.* **8**, 902 (2008).
77. C. Lee, X. Wei, J.W. Kysar, J. Hone, *Science* **321**, 385 (2008).
78. V. Alzari, D. Nuvoli, S. Scognamillo, M. Piccinini, E. Gioffredi, G. Malucelli, S. Marceddu, M. Sechi, V. Sanna, A. Mariani, *J. Mater. Chem.* **21**, 8727 (2011).
79. Y. Wang, Z. Shi, J. Fang, H. Xu, J. Yin, *Carbon* **49**, 1199 (2011).
80. S. Ansari, A. Kelarakis, L. Estevez, E.P. Giannelis, *Small* **6**, 205 (2010).
81. H. Wang, Q. Hao, X. Yang, L. Lu, X. Wang, *Nanoscale* **2**, 2164 (2010).
82. X. Yang, L. Li, S. Shang, X.M. Tao, *Polymer* **51**, 3431 (2010).
83. X. Zhao, Q. Zhang, D. Chen, P. Lu, *Macromolecules* **43**, 2357 (2010).
84. H. Yang, Q. Zhang, C. Shan, F. Li, D. Han, L. Niu, *Langmuir* **26**, 6708 (2010).
85. K.S. Choi, F. Liu, J.S. Choi, T.S. Seo, *Langmuir* **26**, 12902 (2010).
86. H. Bai, C. Li, X. Wang, G. Shi, *Chem. Commun.* **46**, 2376 (2010).
87. J. Li, S. Guo, Y. Zhai, E. Wang, *Anal. Chim. Acta* **649**, 196 (2009).
88. J. Liang, Y. Huang, L. Zhang, Y. Wang, Y. Ma, T. Guo, Y. Chen, *Adv. Funct. Mater.* **19**, 2297 (2009).
89. J.L. Vickery, A.J. Patil, S. Mann, *Adv. Mater.* **21**, 2180 (2009).
90. H.M. Kim, J.K. Lee, H.S. Lee, *Thin Solid Films* **519**, 7766 (2011).
91. C.M. Santos, M.C.R. Tria, R.A.M.V. Vergara, K.M. Cui, R. Pernites, R.C. Advincula, R. Aileen, M.V. Vergara, *Macromol. Chem. Phys.* **212**, 1 (2011).
92. B. Das, K. Eswar Prasad, U. Ramamurty, C.N.R. Rao, *Nanotechnology* **20**, 125705 (2009).
93. S. Mohamadi, N. Sharifi-Sanjani, *Polym. Compos.* **32**, 1451 (2011).
94. S. Stankovich, D.A. Dikin, G.H.B. Dommett, K.M. Kohlhaas, E.J. Zimney, E.A. Stach, R.D. Piner, S.T. Nguyen, R.S. Ruoff, *Nature* **442**, 282 (2006).
95. M. Fang, K. Wang, H. Lu, Y. Yang, S. Nutt, *J. Mater. Chem.* **19**, 7098 (2009).
96. A.L. Higginbotham, J.R. Lomeda, A.B. Morgan, J.M. Tour, *ACS Appl. Mater. Interfaces* **1**, 2256 (2009).
97. Y. Wang, D. Kurunthu, G.W. Scott, C.J. Bardeen, *J. Phys. Chem. C* **114**, 4153 (2010).
98. W. Hong, Y. Xu, G. Lu, C. Li, G. Shi, *Electrochem. Commun.* **10**, 1555 (2008).
99. J. Yu, P. Jiang, C. Wu, L. Wang, X. Wu, *Polym. Compos.* **32**, 1483 (2011).
100. G.L. Li, G. Liu, M. Li, D. Wan, K.G. Neoh, E.T. Kang, *J. Phys. Chem. C* **114**, 12742 (2010).
101. J. Li, H. Xie, Y. Li, J. Liu, Z. Li, *J. Power Sources* **196**, 10775 (2011).
102. J. Liu, L. Tao, W. Yang, D. Li, C. Boyer, R. Wuhrer, F. Braet, T.P. Davis, *Langmuir* **26**, 10068 (2010).
103. H.J. Salavagione, G. Martínez, M.A. Gómez, *J. Mater. Chem.* **19**, 5027 (2009).
104. Z. Xu, C. Gao, *Macromolecules* **43**, 6716 (2010).
105. H. Hu, X. Wang, J. Wang, L. Wan, F. Liu, H. Zheng, R. Chen, C. Xu, *Chem. Phys. Lett.* **484**, 247 (2010).
106. H. Kim, Y. Miura, C.W. Macosko, *Chem. Mater.* **22**, 3441 (2010).
107. G. Eda, M. Chhowalla, *Nano Lett.* **9**, 814 (2009).
108. N.G. Spitsina, A.S. Lobach, M.G. Kaplunov, *High Energy Chem.* **43**, 552 (2010).
109. J. Lu, I. Do, L.T. Drzal, R.M. Worden, I. Lee, *ACS Nano* **2**, 1825 (2008).
110. K. Zhou, Y. Zhu, X. Yang, J. Luo, C. Li, S. Luan, *Electrochim. Acta* **55**, 3055 (2010).
111. H. Fan, L. Wang, K. Zhao, N. Li, Z. Shi, Z. Ge, Z. Jin, *Biomacromolecules* **11**, 2345 (2010).
112. X. Yang, Y. Tu, L. Li, S. Shang, X.M. Tao, *ACS Appl. Mater. Interfaces* **2**, 1707 (2010).
113. D.D. Kulkarni, I. Choi, S.S. Singamaneni, V.V. Tsukruk, *ACS Nano* **4**, 4667 (2010).
114. D. Cai, M. Song, C. Xu, *Adv. Mater.* **20**, 1706 (2008).
115. T.K. Hong, D.W. Lee, H.J. Choi, H.S. Shin, B.S. Kim, *ACS Nano* **4**, 3861 (2010).
116. Y.K. Kim, D.H. Min, *Langmuir* **25**, 11302 (2009).
117. V.C. Tung, L.M. Chen, M.J. Allen, J.K. Wassei, K. Nelson, R.B. Kaner, Y. Yang, *Nano Lett.* **9**, 1949 (2009).
118. X. Liu, L. Pan, T. Lv, G. Zhu, Z. Sun, C. Sun, *Chem. Commun.* **47**, 11984 (2011).
119. J. Kim, H. Im, J.M. Kim, J. Kim, *J. Mater. Sci.* **47**, 1418 (2011).
120. X.Y. Zhang, H.P. Li, X.L. Cui, Y. Lin, *J. Mater. Chem.* **20**, 2801 (2010).
121. H. Xiang, K. Zhang, G. Ji, J.Y. Lee, C. Zou, X. Chen, J. Wu, *Carbon* **49**, 1787 (2011).
122. H. He, C. Gao, *ACS Appl. Mater. Interfaces* **2**, 3201 (2010).
123. Z.S. Wu, W. Ren, D.W. Wang, F. Li, B. Liu, H.M. Cheng, *ACS Nano* **4**, 5835 (2010).
124. L. Ji, Z. Tan, T.R. Kuykendall, S. Aloni, S. Xun, E. Lin, V. Battaglia, Y. Zhang, *Phys. Chem. Chem. Phys.* **13**, 7170 (2011).
125. B. Zhao, G. Zhang, J. Song, Y. Jiang, H. Zhuang, P. Liu, T. Fang, *Electrochim. Acta* **56**, 7340 (2011).
126. D. Zhang, X. Liu, X. Wang, *J. Inorg. Biochem.* **105**, 1181 (2011).
127. F. Zou, Y. Yu, N. Cao, L. Wu, J. Zhi, *Scripta Mater.* **64**, 621 (2011).
128. W.P. Xu, L.C. Zhang, J.P. Li, Y. Lu, H.H. Li, Y.N. Ma, W.D. Wang, S.H. Yu, *J. Mater. Chem.* **21**, 4593 (2011).
129. B. Li, H. Cao, G. Yin, Y. Lu, J. Yin, *J. Mater. Chem.* **21**, 10645 (2011).
130. H. Chang, Z. Sun, K.Y.F. Ho, X. Tao, F. Yan, W.M. Kwok, Z. Zheng, *Nanoscale* **3**, 258 (2011).
131. X. Yang, M. Xu, W. Qiu, X. Chen, M. Deng, J. Zhang, H. Iwai, E. Watanabe, H. Chen, *J. Mater. Chem.* **21**, 8096 (2011).
132. S. Chen, J. Zhu, X. Wang, *J. Solid State Chem.* **184**, 1393 (2011).
133. F.A. He, J.T. Fan, F. Song, L.M. Zhang, H.L.W. Chan, *Nanoscale* **3**, 1182 (2011).
134. H. HongKun, G. Chao, *Sci. Chin. Chem.* **54**, 397 (2011).
135. P. Guo, G. Zhu, H. Song, X. Chen, S. Zhang, *Phys. Chem. Chem. Phys.* **13**, 17818 (2011).
136. G. Wang, B. Wang, X. Wang, J. Park, S. Dou, H. Ahn, K. Kim, *J. Mater. Chem.* **19**, 8378 (2009).
137. K. Zhang, H. Wang, X. He, Z. Liu, L. Wang, L. Gu, H. Xu, P. Han, S. Dong, C. Zhang, J. Yao, G. Cui, L. Chen, *J. Mater. Chem.* **21**, 11916 (2011).
138. L. Deng, G. Zhu, J. Wang, L. Kang, Z.H. Liu, Z. Yang, Z. Wang, *J. Power Sources* **196**, 10782 (2011).
139. Y. Sun, X. Hu, W. Luo, Y. Huang, *ACS Nano* **5**, 7100 (2011).
140. H. Wang, L.F. Cui, Y. Yang, H.S. Casalongue, J.T. Robinson, Y. Liang, Y. Cui, H. Dai, *J. Am. Chem. Soc.* **132**, 13978 (2010).
141. S.M. Paek, E. Yoo, I. Honma, *Nano Lett.* **9**, 72 (2009).
142. Y. Qiu, K. Yan, S. Yang, L. Jin, H. Deng, W. Li, *ACS Nano* **4**, 6515 (2010).
143. B. Wang, X.L. Wu, C.Y. Shu, Y.G. Guo, C.R. Wang, *J. Mater. Chem.* **20**, 10661 (2010).
144. X. Liu, L. Pan, T. Lv, T. Lu, G. Zhu, Z. Sun, C. Sun, *Catal. Sci. Technol.* **1** 1189 (2011).
145. Y.T. Liang, B.K. Vijayan, K.A. Gray, M.C. Hersam, *Nano Lett.* **11**, 2865 (2011).
146. J. Lu, J.X. Yang, J. Wang, A. Lim, S. Wang, K.P. Loh, *ACS Nano* **3**, 2367 (2009).
147. C. Ling, G. Setzler, M.W. Lin, K.S. Dhindsa, J. Jin, H.J. Yoon, S.S. Kim, M. Cheng, N. Widjaja, Z. Zhou, *Nanotechnology* **22**, 325201 (2011).
148. A.J. Patil, J.L. Vickery, T.B. Scott, S. Mann, *Adv. Mater.* **21**, 3159 (2009).
149. L. Zhang, J. Xia, Q. Zhao, L. Liu, Z. Zhang, *Small* **6**, 537 (2010).
150. M.C. Duch, G.R.S. Budinger, Y.T. Liang, S. Soberanes, D. Urich, S.E. Chiarella, L.A. Campochiaro, A. Gonzalez, N.S. Chandel, M.C. Hersam, G.M. Mutlu, *Nano Lett.* **11**, 5201 (2011). □



https://doi.org/10.1557/mrs.2012.182 Published online by Cambridge University Press



ALDRICH® Materials Science

Materials for Breakthrough Innovations

From Aldrich® Materials Science

Energy

- Thermoelectric materials; Quantum dots, Phosphors; Nanoparticles; Fuel Cell catalysts, Electrodes, Electrolytes

Electronics

- Printed Electronics Inks & Pastes; Materials for OPV, OFET, OLED; Nanodispersions; CNTs & Graphene

Biomedical

- Multifunctional Regenerative Therapy Materials: PEGs, Biodegradable & Natural Polymers; Targeted Drug Delivery: Block copolymers, Dendrimers



Subscribe (free) to:
Material Matters™
aldrich.com/mm

aldrich.com/matsci

©2012 Sigma-Aldrich Co. LLC. All rights reserved. SIGMA, SAFC, SIGMA-ALDRICH, ALDRICH, and SUPELCO are trademarks of Sigma-Aldrich Co. LLC, registered in the US and other countries. FLUKA is a trademark of Sigma-Aldrich GmbH, registered in the US and other countries. Sigma brand products are sold through Sigma-Aldrich, Inc. Purchaser must determine the suitability of the product(s) for their particular use. Additional terms and conditions may apply. Please see product information on the Sigma-Aldrich website at www.sigmaaldrich.com and/or on the reverse side of the invoice or packing slip.

79789
1102

https://doi.org/10.1557/mrs.2012.182 Published online by Cambridge University Press

SIGMA-ALDRICH®